Research Square

Preprints are preliminary reports that have not undergone peer review.
They should not be considered conclusive, used to inform clinical practice,
or referenced by the media as validated information.

Anatomical transformation through the aquatic-terrestrial life-style transition in holometabolous insects

Chenjing Zhao
Taiyuan Normal University
Mengting Huang
Taiyuan Normal University
Feifei Li
Taiyuan Normal University
Xiaowen Li
Taiyuan Normal University
Chengquan Cao
Leshan Normal University
Min Li
Taiyuan Normal University
Tong Wang
Jiangsu Academy of Agricultural Sciences
Ding Yang
China Agricultural University
Xingyue Liu
xingyue_liu@yahoo.com

Chinese Academy of Sciences

Research Article

Keywords: aquatic insects, organ development, metamorphosis, evolution, adaptation

Posted Date: June 18th, 2026

DOI: https://doi.org/10.21203/rs.3.rs-9883253/v1

License: This work is licensed under a Creative Commons Attribution 4.0 International License.
Read Full License

Additional Declarations: No competing interests reported.

Anatomical transformation through the aquatic-terrestrial life-style transition in holometabolous insects

Chenjing Zhao[1#*], Mengting Huang[1#], Feifei Li[1#], Xiaowen Li[1], Chengquan Cao[4], Min Li[1], Tong Wang[5], Ding Yang[3*] & Xingyue Liu[2,3*]

[1] College of Biological Sciences and Technology, Taiyuan Normal University, Jinzhong 030619, China.

[2] State Key Laboratory of Animal Biodiversity Conservation and Integrated Pest Management, Institute of Zoology, Chinese Academy of Sciences, Beijing 100101, China.

[3] Department of Entomology, China Agricultural University, Beijing 100193, China.

[4] College of Life Science, Leshan Normal University, Leshan 614000, China.

[5] Central Laboratory, Jiangsu Academy of Agricultural Sciences, Nanjing 210014, China.

[#]These authors contributed equally.

*Corresponding authors: Chenjing Zhao (zhaochenjing398@126.com); Ding Yang (dyangcau@126.com); Xingyue Liu (xingyue_liu@yahoo.com).

Abstract

Background The adaptation of aquatic insects to freshwater habitats is a key question for understanding insect evolution. Many aquatic insects undergo significant morphological and physiological changes during the aquatic-terrestrial life-style transition. However, changes of internal anatomical structures and organs with the process of transformation have yet to be comprehensively investigated.

Results Here we document the anatomical transformations of the skeletal-muscular system, nervous system, digestive system, and tracheal system during the aquatic-terrestrial life-style transition in an aquatic insect species *Protohermes xanthodes* Navás, 1914 (Megaloptera: Corydalidae), using micro-CT and 3D reconstruction. Notably, unlike the rapid, concentrated breakdown of other organ systems, the tracheal system undergoes a prolonged, stepwise, and tightly orchestrated disintegration-reconstruction process during the major developmental stages. The digestive system is markedly modified but without complete disintegration across these stages. For predation and sensation under water, the larvae possess powerful mandibles and prothoracic muscles, and short but well-developed antennal nerves. In addition, the well-developed mesothoracic, metathoracic, and abdominal muscles at the filament base of the larvae enable underwater swimming.

Conclusions This study provides new insights into the dynamic adaptations during the aquatic-terrestrial transition in insects and sheds light on coordinated evolution across multiple functional systems in response to environmental pressures.

Key words aquatic insects; organ development; metamorphosis; evolution; adaptation

Background

Insects, as the most diverse group of animals, showcase extraordinary morphological diversity and occupy a vast array of ecological niches [1–4]. Throughout their life cycles, insects undergo profound changes in both external morphology and internal structures to adapt to diverse environmental conditions [5–7]. It is well known that many insects, i.e., those classified as aquatic insects, inhabit freshwater habitats at partial stage of their life history. Compared to the terrestrial life-style, the evolution of the aquatic life-style in insects is particularly intriguing, as it requires dramatic changes in morphological, physiological, and behavioral traits associated with locomotor, feeding, and respiratory functions in freshwater habitats.

The aquatic insects have evolved specialized structures that connect to the tracheal system to facilitate oxygen acquisition. In parallel, their overall body morphology is adapted to meet the functional demands of underwater life. These adaptations may include morphological streamlining to reduce hydrodynamic resistance. For example, in certain groups such as the aquatic larvae of Neuroptera (lacewings, e.g., Nevrorthidae [8]) and Mecoptera (scorpionflies, e.g., Nannochoristidae [9]), a flattened head and slender body are present, along with a reduction in body setae. Additionally, many aquatic larvae possess specialized appendages for anchorage in underwater substrates, such as the prolegs on the terminal abdominal segment of Corydalidae [10,11], Gyrinidae [12], Trichoptera [7], and Nannochoristidae [13].

The cephalic nerve appears to exhibit distinct morphological adaptations in response to differing sensory and locomotor demands across habitats. In terrestrial

habitats, larvae usually possess a well-developed brain and balanced neural development in the visual, antennal, and mouthpart region, as seen in green lacewings [14] and mantispid lacewings [15]. In contrast, the aquatic lacewing larvae tend to show a reduction or loss of specific brain structures (e.g., missing optic lobes in *Sisyra* larvae and extremely thin optic nerves in *Nevrorthus* larvae) alongside well-developed antennal nerves [8,16]. A similar morphological trend towards visual reduction has been noted in some subterranean neuropteran larvae, such as *Ithone* and *Dilar* [17,18]. Furthermore, in wood-boring beetle larvae (Coleoptera: Archostemata: Cupedidae), the optic lobes and optic nerves are reported as absent, whereas a pair of well-developed nerve stems, likely corresponding to the antennal nerves, are present in the anteriormost region of the brain [19]. Compared to the clearly documented absence of the optic lobe or the extreme thinning of the optic nerve in these larvae, a distinct, moderate pathway is seen in aquatic *Nannochorista*, where both optic and antennal nerves remain slender [20]. These patterns may be related to the sensory demands of specific environments, where larvae in aquatic, soil, or wood-boring habitats may rely more on mechanical pressure such as water flow, substrate vibration, or tactile exploration. Given that relevant mechanoreceptors are primarily distributed on antennae [21,22], antennal nerves in such taxa may undergo corresponding development to support signal transmission. Conversely, sensory functions like vision appear to be structurally reduced.

In the species with aquatic larval stage and terrestrial adult stage, the critical processes of external and internal structural transformation occur primarily during the

pupal stage. This stage involves extensive remodeling of body structures, enabling exploitation of distinct ecological niches at different life stages. A classic anatomical study by Pilgrim [23] on the scorpionfly species *Choristella philpotti* (Mecoptera: Nannochoristidae) revealed a shift in the respiratory system that progresses from larval apneusty (non-functional spiracles) to hemispiracular respiration in prepupae and finally to full spiracular respiration in pupae and adults. This work provides a key example of respiratory adaptation during a habitat transition. Nevertheless, comprehensive morphological studies that integrate respiratory, locomotor, feeding, and sensory systems across the entire aquatic-terrestrial transformation remain scarce. While some studies have focused on insect metamorphosis in general [14,24–31], specific investigation on the metamorphosis coupled with such environmental shift is largely missing.

The holometabolous insect order Megaloptera is one of the major groups of aquatic insects, with the larvae exclusively inhabiting freshwater habitats, such as streams, ponds, etc. However, the other developmental stages of Megaloptera, i.e., egg, pupa, and adult, are terrestrial. Moreover, there is significant change of the feeding habits in Megaloptera, from the predatory larvae to florisugent or bark-secretion-sucking adults. In adaptation to the aquatic life-style, multiple morphological traits are evolved in larvae, e.g., the abdominal lateral filaments, the ventral tracheal gills, the spiracle tubes, etc. Thus, Megaloptera represents an important model for investigation on the developmental transformation from the aquatic to terrestrial life-style in insects.

Here we employed micro-CT and 3D reconstruction techniques to document the

detailed morphological changes of a megalopteran species *Protohermes xanthodes* Navás, 1914 (Megaloptera: Corydalidae: Corydalinae) across the larval, pupal, and adult stages. We focused on the skeleto-muscular system, head nervous system, tracheal system and digestive system, to figure out their major changes between aquatic and terrestrial life-style. This study will provide novel insights into the morphological and functional adaptations during the development in aquatic insects.

Results

We reconstructed the 3D structure of the skeleto-muscular, nervous, digestive, and tracheal systems of the larval, prepupal, pupal, and adult stages (overall in lateral view: Fig. 1, dorsal and ventral view: Additional File 1: Fig. S1). We discovered several novel and fascinating internal anatomical transformations within the conversion of aquatic-terrestrial lifestyles. These transformations are initiated during the prepupal stage; they follow a sequential histological process beginning with skeletal elements, progressing through the central nervous system, tracheal system, and digestive system, and concluding with the musculature; these changes include a respiratory shift from the combined use of spiracles (with their tracheae), tracheal gill (with their tracheae), and cuticle in aquatic larvae to the exclusive reliance on the spiracular system in terrestrial adults. The transformation of each organ system is presented below.

3D structures of skeleto-muscular system

The external morphology (overall appearance) of each stage (larva, pupa, adult) is documented in Additional File 2: Note S1. The internal musculature is described as

follows.

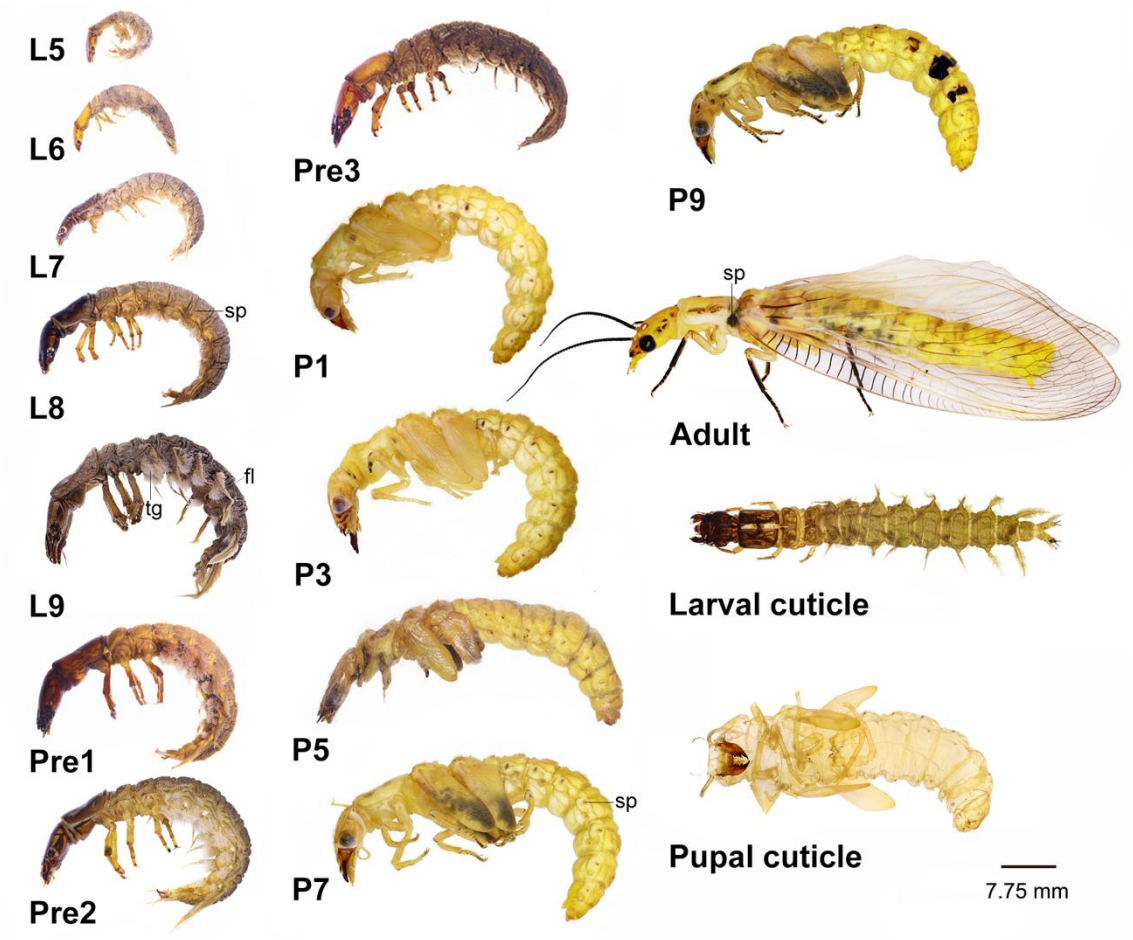


Fig. 1. Overall view of larva, pupa and adult of *Protohermes xanthodes*. Scale bar: 7.75 mm. L5-L9: lateral view of the larva; Pre1-Pre3: lateral view of the prepupal; P1-P9: lateral view of the pupa. Abbreviations: fl: filament; tg: tracheal gill; sp: spiracle.

Larva (Fig. 2: l5–l9). The skeleto-muscular system in 5th instar larvae (Fig. 2: l5) is modest in size, while it becomes significantly larger in the 6th and 7th instars (Fig. 2: l6, l7), and even more robust in the 8th and 9th instars (Fig. 2: l8, l9). The 9th instar larvae possess well-developed cephalic musculature (Fig. 3: larva in A–D), with the detailed origins and insertions of all head muscles provided in Additional File 3: Table S1. Notably, the labrum (such as 0lb1 M. frontolabralis; Fig. 3: larva in A), mandible (which bears four distinct sharp apical incisors, contrasting with the three blunter apical

incisors in adults; see Fig. S2 for comparison; such as 0md1 M. craniomandibularis internus and 0md3 M. craniomandibularis externus posterior; Fig. 3: larva in B), maxilla (such as 0mx1 M. craniocardinalis; Fig. S3: larva in A, B), and pharynx (such as 0ci1 M. clypeopalatalis, 0ph1 M. verticopharyngealis, 0ph2 M. tentoriopharyngealis; Fig. 3: larva in C, D) are all well-musculated. All antennal muscles originate from anterior tentorial arm and insert directly into the base of antenna or the internal scape. The labial muscles are relatively fewer in number, and no muscles attaching to the internal labial palps (Fig. S3: larva in C). The larval prothoracic musculature is generally longer, robust and relatively abundant, with some of the dorsoventral muscles obliquely inserting into the ventral cervical sclerite (Fig. S4: larva in A, B). Mesothoracic muscles, by contrast, are both shorter and fewer, with their dorsoventral muscles inserting vertically into the sternum. Also, the muscles around the meso- and metacoxae are slightly less robust than those around the procoxa. Notably, the ventral longitudinal muscles of the mesothorax are broader and more developed than those of the prothorax (Fig. S4: larva in C).

Transformations during prepupal and pupal stages (Fig. 2: pre1-p9). The transformation of muscles from larva to adult primarily occurs during the prepupal stage, with extensive histolysis and reconstruction of the skeletal and muscular structures, which then continue to develop gradually until the adult stage is reached. This dynamic process is exemplified by the mandibular muscles (0md1, 0md3; Fig. S5). On the first day of the prepupal stage, most muscles undergo disintegration, persisting as amorphous masses (Fig. 2: pre1). By the second day, the inner cuticle is compressed,

and muscles continue to disintegrate (Fig. 2: pre2). By the third day, skeletal structures begin to form, and new muscle fibers appear. In the following days, more and more muscle fibers and bundles emerge (Fig. 2: pre3–p9).

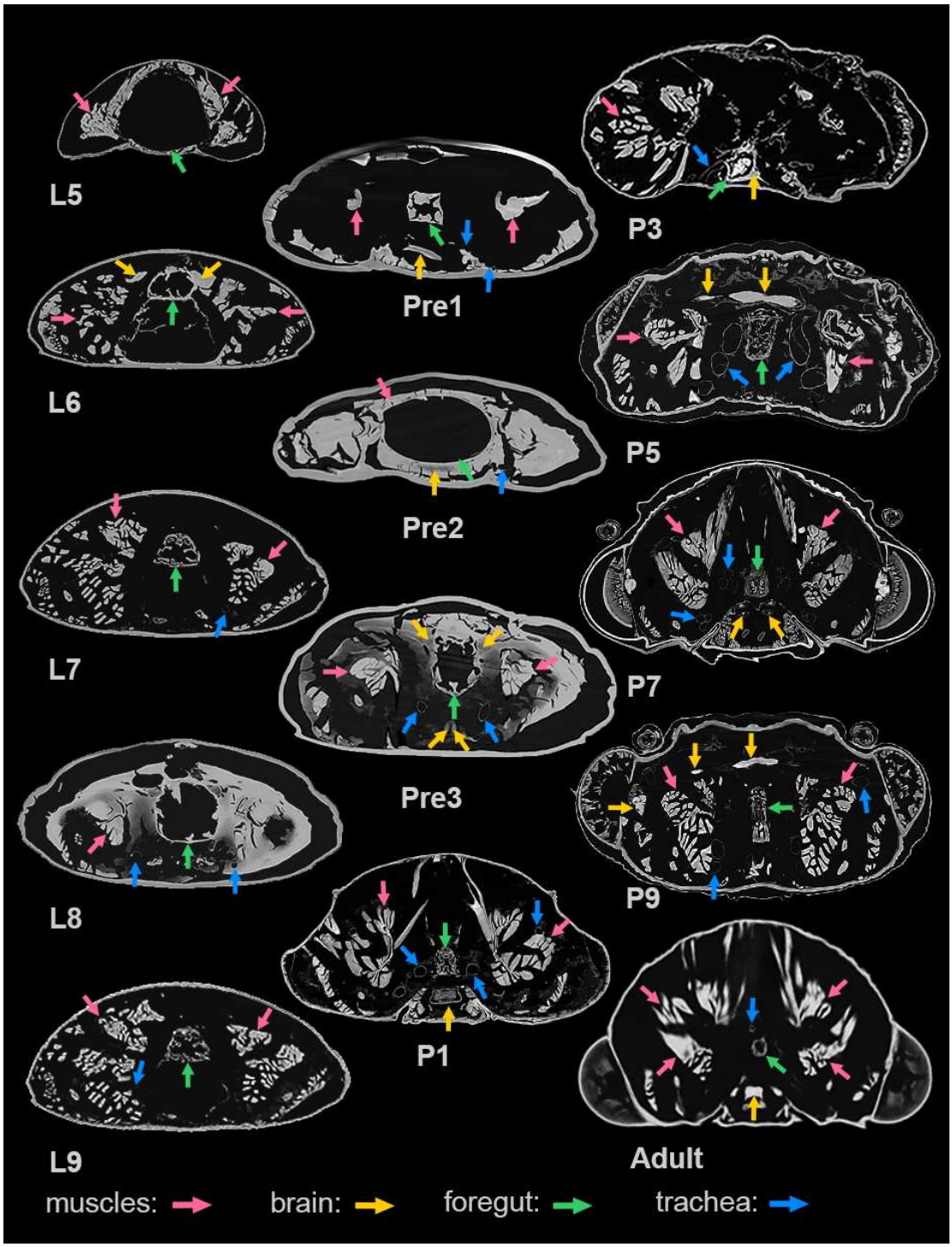


Fig. 2. *Protohermes xanthodes* cross sections from micro-CT of head from pupae to adults. Muscle fibers in pink arrow, nerves in yellow arrow, foregut in green arrow.

The pupal musculature of day 9 is presented as detailed 3D reconstructions (Fig. 3: pupa in A–D). It generally resembles the adult form but remains incompletely developed. The origins and insertions of these pupal head muscles are detailed in Table S2. Specifically, certain muscles are not yet fully attached to the skeleton (such as 0bu4 M. tentoriobuccalis lateralis posterior), and some smaller muscles remain undeveloped (such as 0mx10 M. stipitopalpalis internus). The musculature of pupal head is illustrated, including muscles of antenna (Fig. 3: pupa in A), labrum (Fig. 3: pupa in A), mandible (Fig. 3: pupa in B), maxilla (Fig. S3: pupa in A, B), labium (Fig. S3: pupa in C), and pharynx (Fig. 3: pupa in C, D). In the thorax, the prothoracic muscles are slender and fewer; conversely, the mesothoracic muscles are more robust and abundant. The tergopleural and sternopleural muscles also develop relatively later. The musculature of pupal thorax, including cervical, prothoracic, and mesothoracic muscles, is shown in Fig. S4.

Adult (Fig. 2: adult). The head muscles in adults have formed into distinct bundles (Fig. 2: adult) and develop well (Fig. 3: adult in A–D), with their attachments and presumed functions provided in Table S3. The homologies of these muscles across larval, pupal, and adult stages are summarized in Table S4. While the antennal flagella still lack the intrinsic muscles (Fig. 3: adult in A), adults develop intrinsic muscles in both the maxillary palps (Fig. S3: adult in A, B) and labial palps, along with three novel pairs of labial muscles (Fig. S3: adult in C): M. praementolingulalis posterior (0la11), M. praementolingulalis anterior (0la12), and M. praementopalpalis externus (0la14). The first two (0la11and 0la12) have not been found in other groups of Neuropterida

(see Table S5). Functionally, 0la11 and 0la12 facilitate the movement of the labium, whereas 0la14 controls the labial palps. Given the fusion of the glossa and paraglossa into a ligula in *P. xanthodes*, we infer that this fusion has led to a shift in muscle attachment sites. Consequently, we consider M. praementoligulalis posterior and M. praementoligulalis anterior to be homologous with M. praementoparaglossalis and M. praementoglossalis (described by Wipfler et al. [32]), respectively. The mandibular muscles are slightly smaller than those in the larva (Fig. 3: adult in B), while the pharyngeal muscles are distinctly more slender (Fig. 3: adult in C, D). The pterothoracic muscles are far more robust and abundant than the prothoracic muscles (Fig. S4: adult in A, B). This is particularly pronounced in dorsal longitudinal, dorsoventral, tergopleural, and sternopleural muscles. In contrast, the ventral longitudinal muscles are relatively more slender than those in larvae (Fig. S4: adult in C).

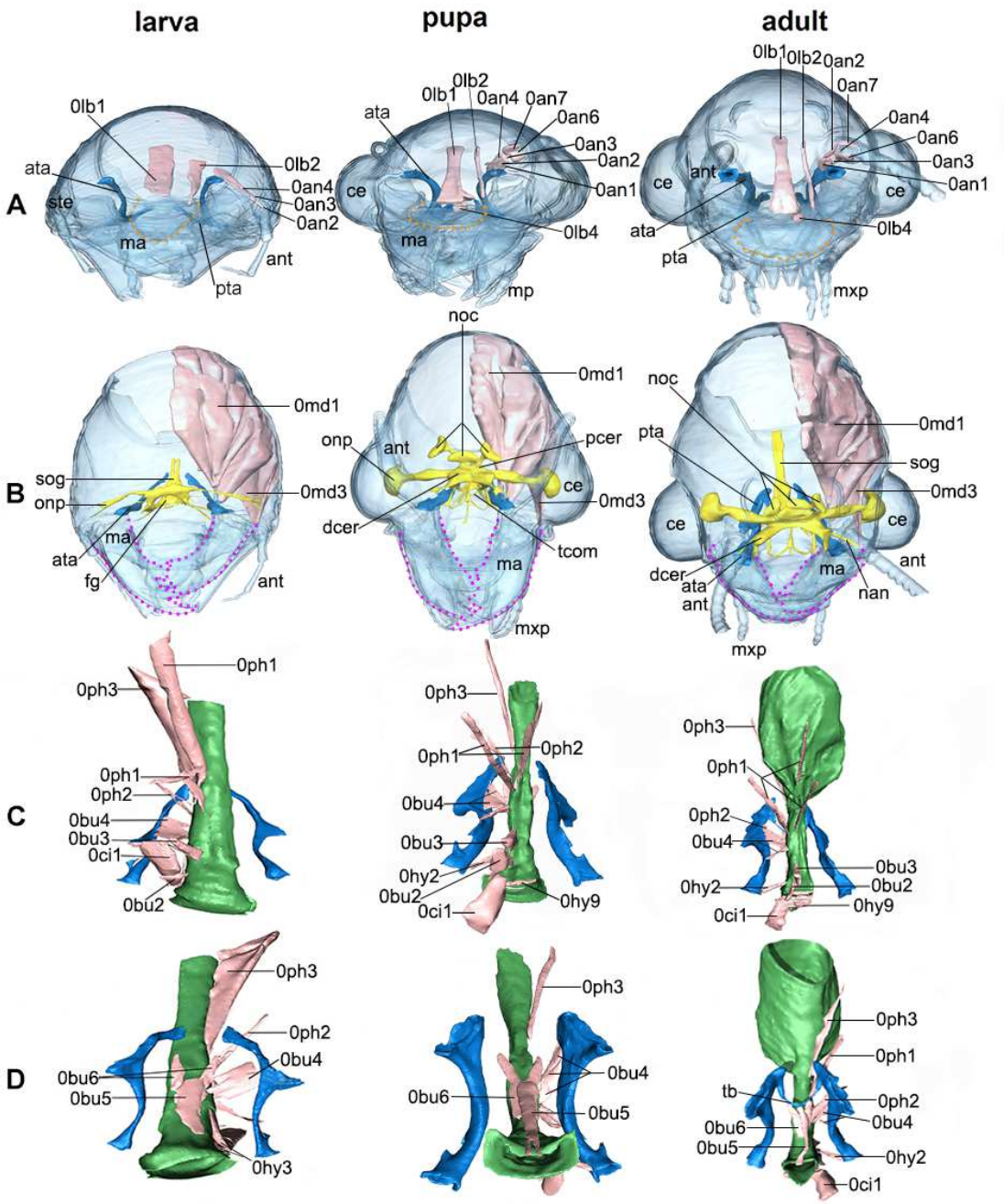


Fig. 3. *Protohermes xanthodes,* 3D reconstructions of head internal structures of larvae (9th instar), pupae (day 9), and adults, cuticle rendered transparent, muscles in light pink, pharynx in green, labrum in orange dotted line, and mandible in purple dotted line. **A** Half of labrum and antennal musculature, frontal view. **B** Half of mandible musculature, frontal view. **C** Half of epipharynx, pharynx, and hypopharynx musculature, dorsal view. **D** Same, ventral view. Abbreviations: ata: anterior tentorial

arm; dcer: deutocerebrum; fg: frontal ganglion; nan: nervus antennalis; noc: ocellar nerve; onp: optic neuropils; pcer: protocerebrum; pta: posterior tentorial arm; sog: suboesophageal ganglion; tb: tentorial bridge; tcom: tritocerebral commissure. Muscle numbers are defined in Tables S1–S3.

3D structures of cephalic nervous system

The head nervous system is a highly complex structure, and well-integrated network, primarily composed of the brain, suboesophageal ganglion (the first ganglion of ventral nerve cord), and frontal ganglion.

Larva (Fig. 4: l5-l9). The cephalic nervous system in early-instar larvae (5th and 6th instars; Fig. 4: l5, l6) is highly simplified, consisting only of a small, compact brain and an irregular, plate-like suboesophageal ganglion, with circumoesophageal connectives forming an almost complete ring. By the 7th instar (Fig. 4: l7), the brain undergoes slight expansion and begins to develop short optic nerves, while the mandibular and maxillary nerves become notably elongated and robust. In the 8th instar (Fig. 4: l8), the mouthpart nerves are shortened, and the optic nerves are elongated. By the 9th instar (Fig. 4: l9), the brain and suboesophageal ganglion are both well-developed and together occupy approximately one-sixth of the larval head capsule's volume. The protocerebrum features slight lateral enlargements and a shallow central depression, with its two ends connected by very thin optic nerves. Optic lobes are absent. The deutocerebrum gives rise to the antennal nerve, which originates from the paired antennal lobes and extends anteriorly. The frontal connectives originate from tritocerebrum and are extremely thin. The circumoesophageal connectives are well-

developed and continuous with tritocerebrum. The suboesophageal ganglion is a wedge-shaped structure below the pharynx, broad anteriorly and tapering posteriorly. Its anterior portion gives rise to the mouthparts nerve roots (labial, mandibular, and maxillary nerves), while its narrowed posterior end is continuous with the ventral nerve cord.

Transformations during prepupal and pupal stages (Fig. 4: pre1–p9). Unlike the skeleton-muscular system, which undergoes extensive disintegration, the central nervous system undergoes significant morphological changes during the prepupal stage. At day 1 (Fig. 4: pre1), the brain becomes small and simple. Antennal nerves, optic nerves, mouthparts nerves and frontal ganglion are largely disintegrated, while suboesophageal ganglion remains connected with brain via circumoesophageal connectives. By day 2 (Fig. 4: pre2), brain strongly compressed, and the cephalic nervous system disintegrates into a simple ring. By day 3 (Fig. 4: pre3), the brain progressively expands. At the same time, the mandibular and maxillary nerves reappear. After pupation (Fig. 4: p1–p9), antennal nerves become elongated and slender, the frontal ganglion is distinctly present, and the neural pathway to the compound eyes, and ocelli develops progressively.

Adult (Fig. 4: adult). The volume of the cephalic nervous system increases substantially, occupying approximately one-quarter of the head capsule. The protocerebrum is dumbbell-shaped with significantly enlarged lateral optic lobes. Three ocellar nerves extend dorsally from the protocerebrum. The deutocerebrum undergoes substantial expansion, forming a square-like structure that gives rise to two prominent

antennal nerves. The suboesophageal ganglion is nearly rectangular and the frontal ganglion is elongated and triangular, connected through two curved frontal connectives.

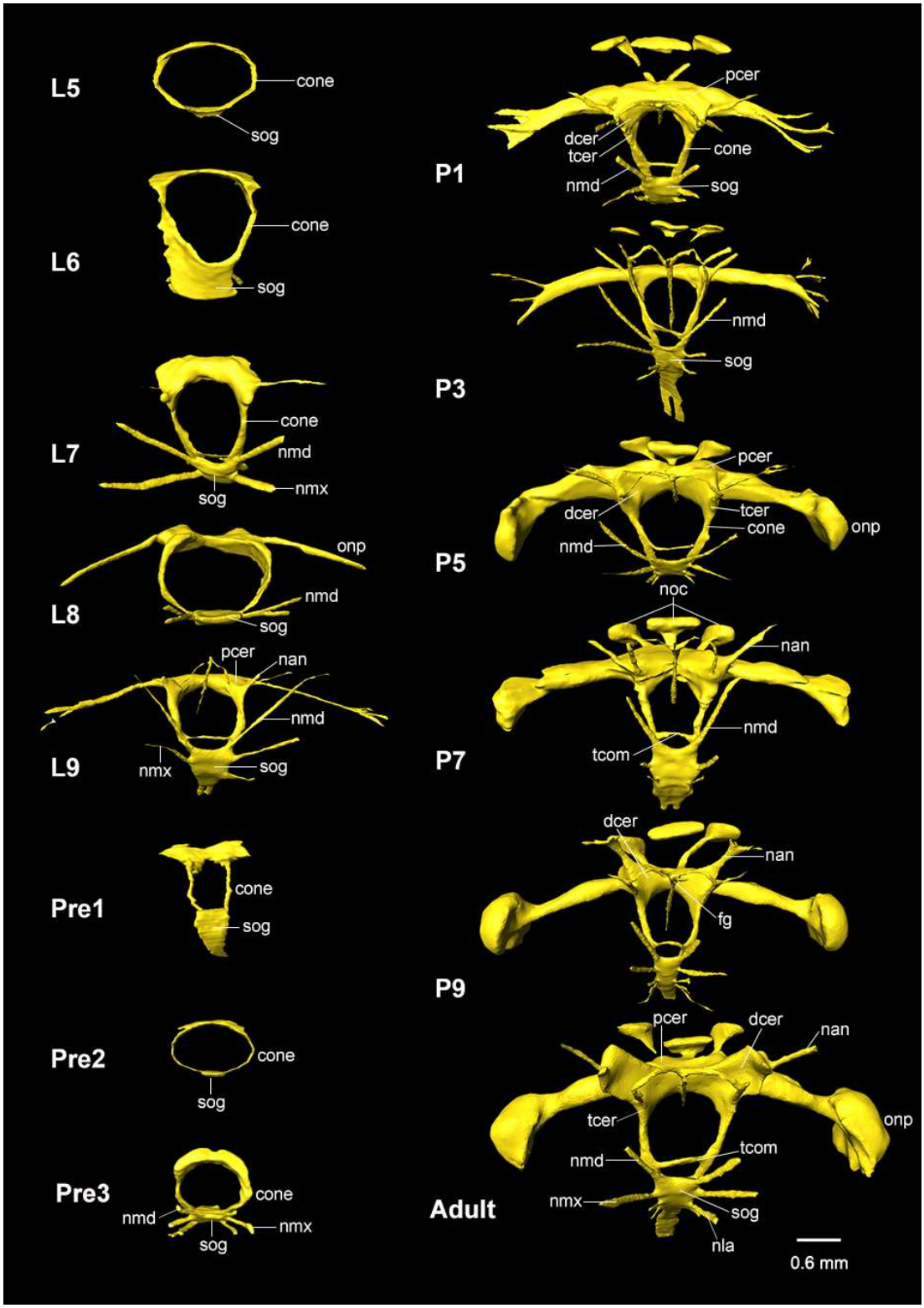


Fig. 4. *Protohermes xanthodes,* 3D reconstructions of cephalic nervous system from

larvae to adults in front view. Scale bar: 0.6 mm. Abbreviations: cone: circumoesophageal connective; dcer: deutocerebrum; fg: frontal ganglion; nan: nervus antennalis; nla: nervus labialis; nmd: nervus mandibularis; nmx: nervus maxillaris; noc: ocellar nerve; onp: optic neuropils; pcer: protocerebrum; sog: suboesophageal ganglion; tcer: tritocerebrum; tcom: tritocerebral commissure.

3D structures of digestive system

Larva (Fig. 5: l5–l9). The digestive tract progressively elongates and thickens with the development of larvae. Within the head, the pharynx and oesophagus are relatively wide (Fig. 5: l5, l6). The pharyngeal opening is large, and the anterior end of the pharynx has a nearly square cross-section. The pharynx extends anteriorly on both sides, connecting to the food passage formed by the mandibles and maxillae. This cephalic portion of the foregut maintains a relatively regular, straight structure and gradually narrows posteriorly (Fig. 5: l7, l8). In the 9th instar larva (Fig. 5: l9), two salivary ducts are present, each connected to a salivary gland. The salivary glands do not enlarge significantly. Each duct folds dorsally over the foregut and extends anteriorly along the lateral sides of the foregut. Throughout the larval stage, the crop gradually expands. From the 6th instar onwards, the gastric caeca of the anterior midgut become apparent. Their size increases with development, and they are typically positioned within the first to third abdominal segments. Meanwhile, the hindgut thickens and elongates, with the ileum and colon maintaining a consistent diameter.

Transformations during prepupal and pupal stages (Fig. 5: pre1–p9). Throughout the prepupal and pupal stages, the digestive tract remains non-histolytic. During the

early prepupal stage (Fig. 5: pre1–pre3), its overall shape appears slender. The salivary ducts and glands undergo complete disintegration, while the crop and gastric caeca experience significant shrinkage. After pupation (Fig. 5: p1), the foregut is noticeably prolonged. By the day 3 (Fig. 5: p3), the crop begins to expand. In contrast, the gastric caeca, which had reached their maximum size at day 1, gradually shrink thereafter. From day 5 onward (Fig. 5: p5–p9), the salivary ducts and glands reappear and progressively develop. Concurrently, both the midgut and hindgut undergo substantial enlargement throughout the pupal stage. The hindgut continues to elongate, with the ileum forming distinct folds.

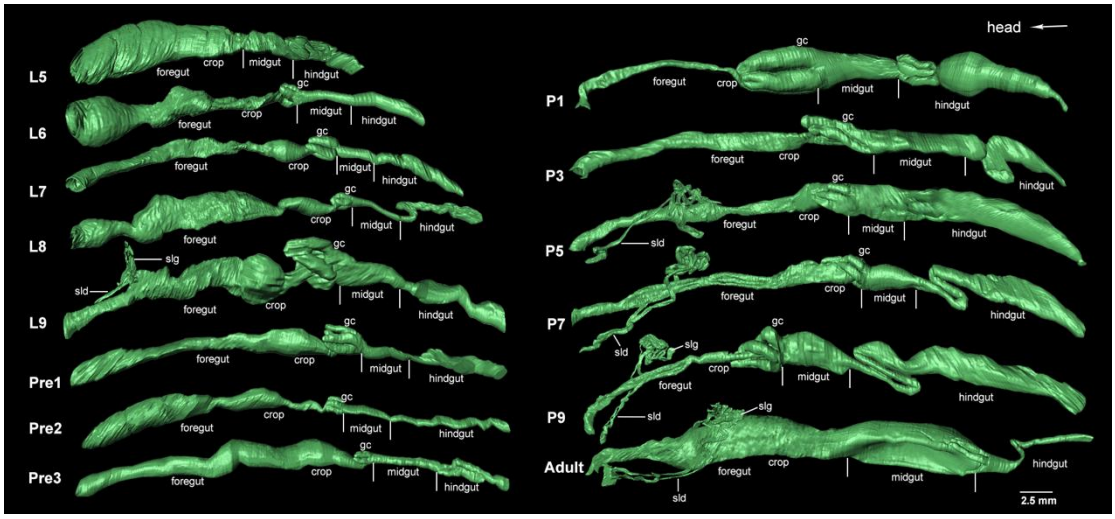


Fig. 5. *Protohermes xanthodes*, 3D reconstructions of digestive system from larvae to adults: lateral view. Scale bar: 2.5 mm. Abbreviations: gc: gastric caeca; sld: salivary duct; slg: salivary gland.

Adult (Fig. 5: adult). The digestive tract shows a marked change in diameter. The section near the brain remains relatively narrow, while the portion closer to the posterior head is abruptly widened, reaching a diameter nearly double that of the anterior segment. The salivary ducts are notably elongated, and the salivary glands are fully developed

and considerably enlarged. Additionally, the crop is significantly expanded, and the midgut is both thickened and elongated. Notably, the gastric caeca are absent in adult. Posteriorly, the hindgut is gradually narrowed, and lacks the distinct ileal folds. The colon and rectum remain short and slender.

3D structures of tracheal system

Each side of the body contains two lateral longitudinal trunks, which are interconnected by three branches in the thorax. The lateral longitudinal trunk in the thoracic region is relatively thick and has fewer branches, whereas those in the head and abdomen regions are slightly thinner, with a more intricate branching pattern. An overall model of the tracheal system of thorax and abdomen across life stages is provided in Fig. 6A.

Larva (Fig. 6A: larva, Fig. 6B: l9). Two pairs of distinct lateral longitudinal tracheal trunks are present. One pair is short, extending from the head to the first abdominal segment where it terminates, thereby connecting the spiracular tracheae from the prothorax to the first abdominal segment. The other pair is long, running continuously from the head to the abdomen, linking the spiracular tracheae from the 2nd to the 8th abdominal segment (Fig. 6A: larva, Fig. 6B: l9, Fig. S6: l5–l9). Within the larval head, the main tracheal trunks give rise to numerous long, narrow branches that are intricately distributed among the muscles and nerves. In contrast, each abdominal segment contains one spiracular trachea and two primary tracheae located at the base of the tracheal gill tuft (Fig. 6A: larva). What's more, we found that each tracheal gill is controlled by two muscles. The first is a large retractor muscle originating from the tergal lateral edge and inserting at the gill base via three branches and the second is a

smaller protractor muscle originating near the same region and inserting on the cuticular ridge anterior to the gill base (red arrows in Fig. 6C–F). Similarly, each abdominal segment contains two muscles at the lateral filament bases, though no trachea were observed in the filament. One originates from the lateral edge of the sternum and inserts at the dorsal base of the filament, and another thinner muscle extends from the sternal margin to the base of the filament (orange arrows in Fig. 6C–F). A unique feature of the 8th abdominal segment is the absence of a tracheal gill, leaving it with only a spiracular trachea. Additionally, each abdominal segment possesses two dorsal and two ventral tracheal branches (dt, vt; Fig. 6A: larva, Fig. 6B: l9), which extend to the muscles, nerves, and digestive tract. Moreover, in late-instar larvae, a ventral tracheal commissure (vtc; Fig. 6A: larva, Fig. 6B: l9, Fig. S6: l8, l9) connects the two short lateral longitudinal trunks in each thoracic segment and the first abdominal segment. In the 2nd to 7th abdominal segments, a similar ventral commissure connects the two long lateral longitudinal trunks, though in some segments it is difficult to recognize or cannot be traced. In addition, in the first five abdominal segments, a small tracheal branch links the gill tuft trachea of each segment to the spiracular trachea of the next segment (tts; Fig. 6A: larva, Fig. 6B: l9, Fig. S6: l8, l9).

Transformations during prepupal and pupal stages (Fig. 6A: early prepupa, Fig. 6B: pre3, Fig. S6: pre1–p9). During the prepupal and pupal stages, the primary tracheal trunk undergoes only a slight increase in size. However, extensive remodeling occurs in many of its branch networks. Upon entering the prepupal stage (Fig. S6: pre1, pre2), the larva exhibits increased tracheal branches in the head and thorax, while

abdominal branches are significantly reduced. By day 3 (Fig. 6A: early prepupa, Fig. 6B: pre3), the dorsal and ventral tracheal branches in the abdomen have completely disintegrated. Subsequently, several new dorsal and ventral tracheal branches begin to emerge (Fig. S6: pre5). After day 9, in late prepupae (Fig. S6: pre9), the tracheae at the base of the gill tuft in 6th and 7th segments disintegrate. And the originally short lateral longitudinal trunk elongates toward the 8th abdominal segment through the formation of new tracheae (indicated by red arrows in Fig. 6B: pre11 and Fig. S6: pre9, pre11). This elongation is achieved through a segmental process: new tracheae from the posterior segment's spiracular base grow forward to connect with the preceding segment's spiracular base (e.g., growing forward from segment III to segment II; illustrated by red dashed arrows in Fig. 6A: late prepupa), thereby forming a continuous trunk across the abdomen during the following prepupal days. By day 11, the gill tuft tracheae (tbt) of the first five segments, along with their connecting tracheae (tts) disappear completely. Thereafter, entering the pupal stage (Fig. S6: p1), only the spiracular trachea remains in each abdominal segment. The originally short lateral longitudinal trunk is now fully elongated into a continuous trunk reaching the posterior end of the abdomen. By day 3 (Fig. S6: p3), the dorsal tracheal commissures (dtc) first appear in the abdominal segments, whereas the ventral tracheal commissures in the abdomen cannot be observed in the CT data. In contrast, those in the thoracic region remain intact and clearly visible. Additionally, the dorsal and ventral branches (dt, vt) increase in number during the late pupal stage (Fig. 6A: pupa, Fig. 6B: p7).

Adult (Fig. 6A, B: adult). In the adult, the tracheal system closely resembles that of

the late pupae, although the tracheal junctions appear notably thicker.

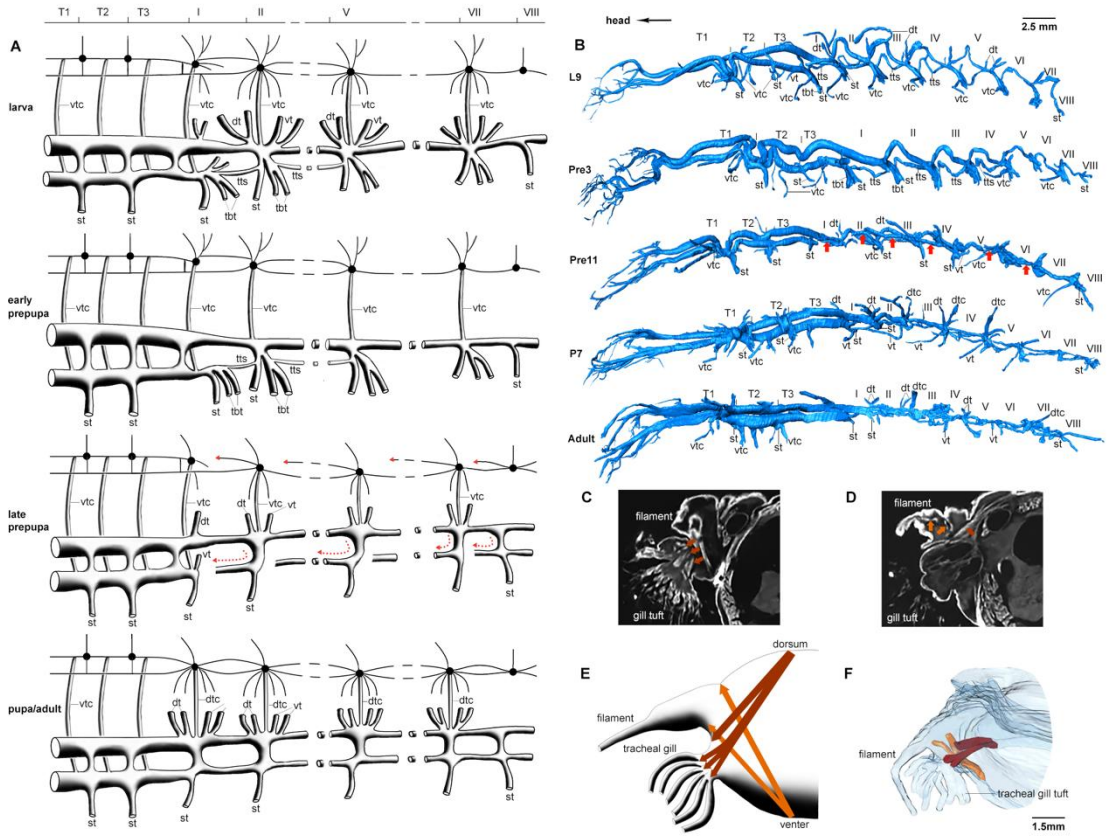


Fig. 6. *Protohermes xanthodes*, tracheal system from larvae to adults: dorsal view. **A** Overall model of the tracheal system of thorax and abdomen for *Protohermes xanthodes*: larva, early prepupa, pupae, and adults. The red dashed arrows indicate the direction of new tracheal growth. **B** 3D reconstructions of tracheal system from specimens consistent with the overall model in morphology. Red arrows indicate the new tracheae growing from the spiracle tracheal base, which serve to elongate the initially short lateral longitudinal trunk. Scale bar: 2.5 mm. **C** Micro-CT cross sections of tracheal gill. Red arrows indicate the retractor muscles of tracheal gill. Scale bar: 1.5 mm. **D** Micro-CT cross sections of filament and tracheal gill. Orange arrows indicate the muscles of filament and red arrow indicates the protractor muscles of tracheal gill. **E** Overall model of muscles of the tracheal gill and filament for *Protohermes xanthodes*. **F** 3D

reconstructions. Abbreviations: dt: dorsal trachea; dtc: dorsal tracheal commissure; st: spiracle trachea; T1–T3: prothorax, mesothorax, metathorax; tbt: trachea at the base of the tracheal gill tuft; tts: tracheal branch connecting the gill trachea and the spiracular trachea; vt: ventral trachea; vtc: ventral tracheal commissure; I–VIII: 1st –8th segment in abdomen.

Discussion

Respiration adaptation to aquatic and terrestrial habitats

The tracheal system of *P. xanthodes* exhibits remarkable morphological adaptations that align with the distinct respiratory demands of aquatic larvae and terrestrial adults. In aquatic larvae, well-developed tracheal gills play an important role in respiration through gas exchange [33,34]. The large retractor muscle of each tracheal gill is consistent with the "single powerstroke muscle" described by Kinnamon & Kammer [35] as being responsible for gill retraction. The smaller protractor muscle likely corresponds to the "protractor muscle (GPM1)" described in the same study. These muscles together regulate the gill movement, allowing rhythmic retractions and protractions of the gill (see Additional File 4: Video S1). Barclay et al. [34] described the rhythmic fanning or pulsing of the tracheal gills, a behavior consistent with promoting gases diffusion across the gill membrane. Similarly, coordinated contraction of the two muscles at the lateral filament bases directs filament movement, which in turn may help maintain aquatic balance and enhance locomotion efficiency (Video S2). Beyond these muscular adaptations, the organization of the tracheal system further

supports respiration through the ventral tracheal commissures in the larval thorax and abdomen, which improve the distribution and circulation of oxygen within the body.

During the transition from aquatic to terrestrial habitats, the tracheal system undergoes a dynamic remodeling process. Initially, in the early prepupal stage after leaving water, the number of tracheal branches increases in the head and thorax but temporarily decreases in abdomen, likely redirecting oxygen toward developing cephalic and thoracic organs. The abdominal tracheal branches soon regenerate and increase gradually in number in the following days, ensuring an adequate oxygen supply to the abdominal organs during the mid-to-late prepupal phase. It is noteworthy that the tracheae at the base of gill tufts (tbt) do not disintegrate until the late prepupal stage. This phenomenon is likely an adaptation to ensure adequate oxygen uptake in the soil, meeting the respiratory demands of the prepupal stage. After entering the pupal stage, the short lateral longitudinal trunks complete their elongation, followed by the reconstruction of the dorsal tracheal commissures. As a result, this remodeling establishes a terrestrial-adapted abdominal tracheal network in the adult, better suited for aerial respiration and reproductive activities such as mating and oviposition. Taken together, unlike the rapid, concentrated breakdown of other organ systems, the tracheal system undergoes a prolonged, stepwise, and tightly orchestrated disintegration-reconstruction process throughout the prepupal and pupal stages.

Morphological adaptation of predation under water

As active predators of aquatic invertebrates, the *P. xanthodes* larvae consume substantial amounts of food for growth. Notably, despite metamorphosis, both larvae

and adults retain prognathous chewing mouthparts, with many muscles remain homologous across life stages (see Table S4). This contrasts sharply with that in Neuroptera, which undergo dramatic transformations in mouthpart morphology, shifting from larval piercing-sucking mouthparts to adult chewing-type mouthparts [8,14,16]. In *P. xanthodes*, the larval pharynx is particularly large, with the diameter comprising approximately 40% of the head capsule width. Correspondingly, the muscles M. verticopharyngealis (0ph1) and M. postoccipitopharyngalis (0ph3) are nearly four times as large as those in some terrestrial larvae [14,27]. These modifications enhance prey processing efficiency in freshwater habitats, supporting the view that robust mouthpart morphology is important for efficient predation under water [36].

Based on our observation, the underwater feeding adaptation is exhibited not only in their robust mandibles, maxillary and associated musculature but also in their well-developed cervical and prothoracic (including the musculature) as well as their robust forelegs, collectively enabling efficient prey processing (see Video S3). The larval cervix and prothorax contain numerous long and robust muscles, which attach ventrally obliquely to the cervix and dorsally to the pronotum. The tergopleural, sternopleural, and pleurocoxal muscles are also distinctly strong. These muscles provide the structural basis for head rotation and forceful feeding. Meanwhile, during feeding, the forelegs contribute to grasp prey. The coxal and femoral muscles are slightly more robust than those of the mid- and hindlegs. All these powerful muscular adaptations provide the necessary force to overcome hydrodynamic resistance during underwater feeding. In

contrast, the muscles of the cervix and prothorax in adults are significantly reduced and slenderer (Fig. S4). Additionally, the muscles of the pharynx and forelegs also become notably finer in adults.

Notably, a sternopleural muscle originates from the anterolateral margin of the coxa and inserts on the lateral part of the lateral cervical sclerite. Present in both the larva and pupa (outlined with a white dashed line in Fig. S4B), this muscle likely functions in rotating the cervix during predation. During the pupal stage, it gradually becomes thinner, suggesting a potential shift in function towards stabilizing the prothoracic pleuron. It is absent in adults, a loss probably due to the increased sclerotization and the reduced demand for forceful predatory movements in the adult stage. Similar findings have been reported in leaf beetles (Chrysomelidae) [27] and *Drosophila melanogaster* [31].

Locomotion and associated structural changes in aquatic and terrestrial habitats

Based on our observations of *P. xanthodes* larvae, their underwater locomotion primarily consists of crawling on rocks and swimming. The swimming posture exhibits an undulating up-and-down motion, resembling the human butterfly stroke, with the main power generated by meso- and metathoracic muscles that drive abdominal undulation. As the primary locomotor center, the meso- and metathorax, although smaller and less muscular than the prothorax, possesses broad and robust dorsal and ventral longitudinal muscles. These muscles assist in fine bending and extension of body segments, providing substantial power for aquatic swimming. Compared to larvae, adults possess significantly more and stronger pterothoracic muscles, except for the

ventral longitudinal muscles, which become finer. These changes are associated with the transition to a terrestrial lifestyle, where the primary mode of locomotion shifts to flight.

Beyond muscular modifications, the shortened, robust antennae of the *P. xanthodes* larvae may be also a distinct aquatic specialization, a morphology convergent in other neuropteran aquatic larvae [8,16]. The antennae are equipped with mechanoreceptor to detect water flow changes. Their short antennal nerves reduce neural transmission distance, allowing faster response speed during predation or escape [37]. In *P. xanthodes* larvae, although optic nerves are present, the optic lobes are absent, a condition similar to that in other aquatic neuropteran larvae, such as *Sisyra* and *Nevrorthus*. This likely represents a neural adaptation to the dimly lit, high hydrodynamic pressure conditions of the aquatic environment. In contrast, as terrestrial adults of *P. xanthodes*, the brain increases in volume, featuring thick, elongate antennal nerves and expanded optic lobes. The protocerebrum acquires a square-shaped morphology, expanding to approximately three times its larval volume. These neural adaptations improve the adults' ability to integrate and process more complex environmental information on land and to generate appropriate locomotion and behavioral responses.

Conclusion

The present study provides an anatomical analysis associated with the aquatic-terrestrial life-style transition in the dobsonfly *Protohermes xanthodes*. The transformation involves sequential and coordinated changes across multiple organ

systems, each adapted to the functional demands of its respective life stage. Larvae use spiracles, tracheal gill, and associated tracheael network for enhanced aquatic respiration. Prepupae and pupae undergo a stepwise process in which the larval tracheae are disintegrated and replaced by adult ones, finally forming an abdominal tracheal network adapted to the terrestrial environment. From larva to pupa to adult, the skeleton-muscular undergoes dramatic remodeling. The robust mandibular, pharyngeal, cervical, prothoracic, and foreleg muscles of the larva progressively degenerate during the prepupal stage. In the adult, the corresponding musculature is markedly reduced and thinner. By contrast, the pterothoracic musculature develops during pupation and becomes numerous and powerful in the adult to support flight (Fig. 7). The digestive and cephalic systems are markedly modified but without complete disintegration across these stages. These findings illustrate the anatomical basis of a major life history transition in insects. Further comparative and interdisciplinary studies will enhance understanding of the evolutionary and developmental mechanisms underlying such transformations.

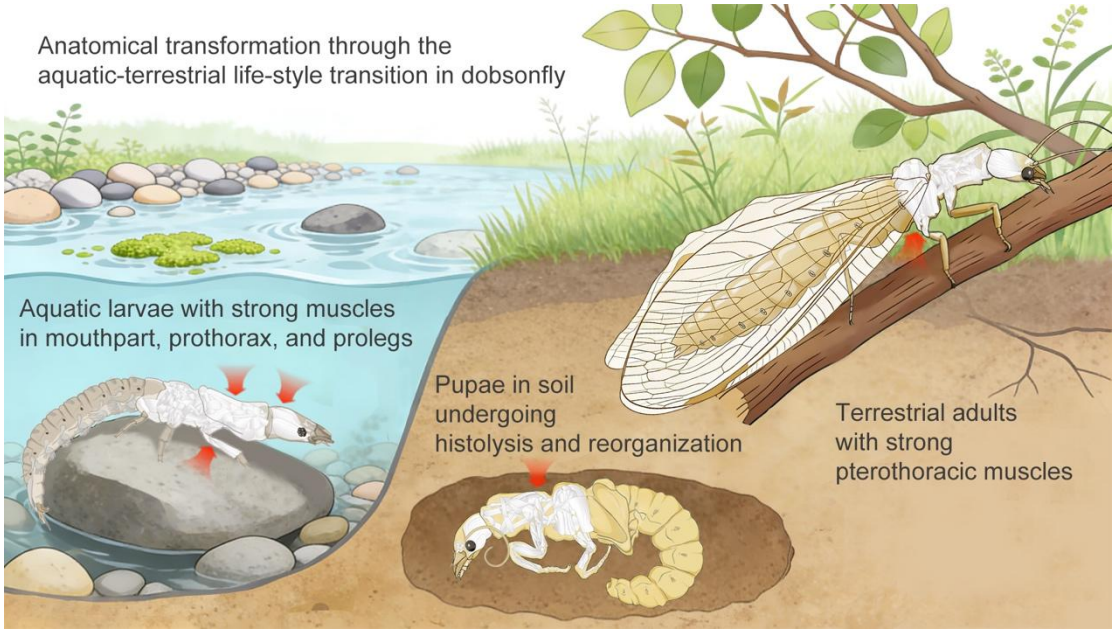


Fig. 7. Overall model of skeleto-muscular remodeling across life stages of *Protohermes xanthodes*: larva (left), pupa (middle), adult (right). The red arrows indicate the labeled representative features in each stage.

Methods

Specimen preparation

We selected *Protohermes xanthodes* Navás, 1914 for the present study because this is a common and widespread species of Megaloptera from East Asia. As a species of the subfamily Corydalinae, the larvae have eight pairs of abdominal lateral filaments and seven pairs of tracheal gills. Four critical life stages were observed: 5th to 9th instar larvae, prepupae, pupae, and adults. The 5th instar larva was obtained from the Insect Resources Research and Development Base in May 2022 from Leshan Normal University. The larvae and adults were fed with *Tenebrio molitor* and kept at a constant temperature of 25 °C, 14 h of light and 10 h of darkness, and a humidity of around 60%. Larvae were sampled for each instar (5th through 9th). Prepupae were collected daily

throughout the 11-day prepupal stage. Pupae were sampled during the 9-day pupal stage at 1, 3, 5, 7, and 9 days after pupation. Adult specimens were collected within 24 h after emergence. Sixty-six specimens were sampled for this study, with three individuals collected per time point or instar, totaling 15 larvae, 33 prepupae, 15 pupae, and 3 adults. All materials were preserved in 75% ethanol for less than 24 h before dehydration.

Microcomputer tomography and computer-based 3D reconstruction

The samples were dehydrated through a gradient ethanol series, sequentially immersed in 75%, 80%, 85%, 90%, 95%, and 100% ethanol, with each step lasting 30 minutes. The dehydrated samples are freeze-dried using a Christ Alpha 2-4 LD plus freeze dryer. The dried specimens were placed on the sample stage of a Zeiss Xradia 620 Versa micro-CT imaging system (beam strength: 40kV-60kV, absorption contrast) to acquire three-dimensional data. The raw micro-CT data were reconstructed using Amira 5.4 to generate the final structure images used for analysis. For the prepupal data, we focused the 3D reconstructions on days 1–3, when the most extensive histolysis and reconstruction occur. In contrast, for the tracheal system, which undergoes a stepwise disintegration, representative data from prepupal day 5, 9, and 11 are included in the figures to document the stepwise remodeling process.

Photography

A series of images at different focal planes were captured using a Canon EOS 80D camera and composited using Helicon Focus 2.0 software to obtain a fully focused final image. All images were processed using Adobe Photoshop 2022 software and arranged for presentation. Larval behavior was recorded digitally.

Terminology

The terminology for skeletal structures generally follows Beutel & Friedrich and Yang & Liu [10,38], while that for muscles follows Friedrich & Beutel and Wipfler et al. [32,39]. Larval specimens were designated by their instar stage, using a prefixed letter to indicate the developmental stage (e.g., l5 for a 5th instar larva). Specimens from prepupal to pupal stages were numbered according to sampling days, with a prefixed letter denoting the stage (e.g., pre1 for a prepupa on the first day after entering the soil, and p1 for a pupa on the first day after pupation).

Abbreviations

dt: dorsal trachea; dtc: dorsal tracheal commissure; tbt: trachea at the base of the tracheal gill tuft; tts: tracheal branch connecting the gill trachea and the spiracular trachea; vt: ventral trachea; vtc: ventral tracheal commissure.

Supplementary information

Additional File 1. Fig. S1: Dorsal view and ventral view of *Protohermes xanthodes.* Fig. S2: *Protohermes xanthodes,* 3D reconstructions of mandibles. Fig. S3: *Protohermes xanthodes,* 3D reconstructions of head internal structures of larvae (9th instar), pupae (day 9), and adults. Fig. S4: *Protohermes xanthodes,* 3D reconstructions of prothorax and mesothorax internal structures of larvae (9th instar), pupae (day 9), and adults. Fig. S5: *Protohermes xanthodes,* 3D reconstructions of mandible muscles (0md1, 0md3) from larvae to adults. Fig. S6: 3D reconstructions of tracheal system

from larvae to adults: lateral view.

Additional File 2. Note S1: The description of external morphology (overall appearance) of each stage (larva, pupa, adult).

Additional File 3. Table S1: Cephalic musculature of the larvae (9th instar) of *Protohermes xanthodes* Navás, 1914. Table S2: Cephalic musculature of the pupae (day 9) of *Protohermes xanthodes* Navás, 1914. Table S3. Cephalic musculature of the adults of *Protohermes xanthodes* Navás, 1914. Table S4: Homologization of the cephalic musculature of *Protohermes xanthodes* Navás, 1914 from larvae to adults. Table S5: Presumed homologies of the cephalic muscles of *Protohermes xanthodes* Navás, 1914 with muscles reported in literatures: *Chrysopa pallens*, *Osmylus fulvicephalus*, *Nevrorthus apatelios*, *Sisyra terminalis*, *Coniopteryx pygmaea*, *Ithone* sp., *Neohermes* sp.

Additional File 4. Video S1: Rhythmic movements of gill tufts during stationary respiration in the final-instar larvae of *Protohermes xanthodes*. Video S2: The swimming video of final-instar larvae of P*rotohermes xanthodes*. Video S3: The feeding and locomotion video of final-instar larvae of *Protohermes xanthodes*.

Acknowledgements

We would like to thank the anonymous reviewers for their valuable feedback, which greatly improved the quality of this manuscript. Additionally, we sincerely thank Suping Wu from the Nanjing Institute of Geology and Palaeontology for assisting with the CT scanning of the samples.

Author contributions

XYL, DY and CJZ conceived and designed the study. CJZ, MTH, CQC and ML analyzed the morphology data. MTH, FFL, XWL and TW carried out experiments. CJZ and MTH wrote the paper. XYL and DY reviewed and edited the manuscript. All authors reviewed the manuscript.

Funding

This study was supported by the National Natural Science Foundation of China (32100359, 32130012), and the Initiative Scientific Research Program (2024IOZ0108) of the Institute of Zoology, Chinese Academy of Science.

Availability of data and materials

All data generated or analyzed during this study are included in this published article.

References

1. Chapman AD. Numbers of Living Species in Australia and the World. 2nd ed. Canberra: Australian Biological Resources Study; 2009.
2. Grimaldi DA, Engel MS. Evolution of the insects. Cambridge: Cambridge University; 2005.
3. Gullan PJ, Cranston PS. The insects: an outline of entomology. 5th ed. Oxford: Wiley-Blackwell; 2014.
4. Goulson D. The insect apocalypse, and why it matters. Curr Biol. 2019;29:R967–

71.

5. Beutel RG, Ribera I, Fikáček M, Vasilikopoulos A, Misof B, Balke M. The morphological evolution of the Adephaga (Coleoptera). Syst Entomol. 2020;45:378–95.
6. Hu F-S, Luo X-Z, Kuan K-C, Beutel RG, Chi K-J, Liu H-C, et al. Ancient divergent evolution of specialized swimming modes in aquatic beetles. P Roy Soc B. 2025;292:20243093.
7. Beutel RG, Goczał J, Pohl H. Evolutionary Adaptations in Larvae of Holometabola. Annu Rev Entomol. 2026;71:149–68.
8. Beutel RG, Friedrich F, Aspöck U. The larval head of Nevrorthidae and the phylogeny of Neuroptera (Insecta). Zool J Linn Soc. 2010;158:533–562.
9. Beutel RG, Hörnschemeyer T. Larval morphology and phylogenetic position of *Micromalthus debilis* LeConte (Coleoptera: Micromalthidae). Syst Entomol. 2002;27:169–90.
10. Yang D, Liu XY. Megaloptera, Insecta vol. 51, Fauna Sinica. Beijing: Science Press; 2010.
11. Yang D, Liu XY, Yang XK. The color atlas of Neuropterida from China. Zhengzhou: Henan Science and Technology Press; 2023.
12. Jäch MA, Beutel RG, Delgado JA, Díaz JA. Hydraenidae Mulsant, 1844. In: Beutel RG, Leschen RAB, editors. Coleoptera, beetles, vol. 1: morphology and systematics (Archostemata, Adephaga, Myxophaga, Polyphaga partim). Berlin: De Gruyter, 2016. p. 228–32.

13. Beutel RG, Friedrich F, Hörnschemeyer T, Pohl H, Hünefeld F, Beckmann F, et al. Morphological and molecular evidence converge upon a robust phylogeny of the megadiverse Holometabola. Cladistics. 2011;27:341–55.
14. Zhao, C, Ang Y, Wang M, Gao C, Zhang K, Tang C, et al. Contribution to understanding the evolution of holometaboly: transformation of internal head structures during the metamorphosis in the green lacewing *Chrysopa pallens* (Neuroptera: Chrysopidae). BMC Evol Biol. 2020;20:79.
15. Jandausch K, Pohl H, Aspöck U, Winterton SL, Beutel RG. Morphology of the primary larva of *Mantispa aphavexelte* Aspöck & Aspöck, 1994 (Neuroptera: Mantispidae) and phylogenetic implications to the order of Neuroptera. Arthropod Syst Phylo. 2018;76:529–60.
16. Jandausch K, Beutel RG, Bellstedt R. The larval morphology of the spongefly *Sisyra nigra* (Retzius, 1783) (Neuroptera: Sisyridae). J Morphol. 2019;280:1742–58.
17. Li D, Friedrich F, Jandausch K, Pohl H, Liu XY, Beutel RG. Unearthing underground predators: the head morphology of larvae of the moth lacewing genus *Ithone* Newman (Neuroptera: Ithonidae) and its functional and phylogenetic implications. Syst Entomol. 2022;47:618–36.
18. Li D, Jandausch K, Pohl H, Yavorskaya MI, Liu XY, Beutel RG. Cephalic anatomy highlights morphological adaptation to underground habitats in a minute lacewing larva of *Dilar* (Dilaridae) and conflicting phylogenetic signal in Neuroptera. Insect Sci. 2023;0:1–19.

19. Yavorskaya MI, Kojima K, Machida R, Beutel RG. Morphology of the first instar larva of *Tenomerga mucida* (Chevrolat, 1829) (Coleoptera: Archostemata: Cupedidae). Arthropod Syst Phylo. 2015;73:239–58.
20. Beutel RG, Kristensen NP, Pohl H. Resolving insect phylogeny: the significance of cephalic structures of the Nannomecoptera in understanding endopterygote relationships. Arthropod Struct Dev. 2009;38:427–60.
21. Seada M, Hamza A. Differential morphology of the sensory sensilla of antennae, palpi, foretarsi and ovipositor of adult *Tribolium castaneum* (Herbst) (Coleoptera:Tenebrionidae). Ann Agr Sci. 2018;63:1–8.
22. Amat C, Marion-Poll F, Navarro Roldán M, Gemeno C. Gustatory function of sensilla chaetica on the labial palps and antennae of three tortricid moths (Lepidoptera: Tortricidae). Sci Rep. 2022;12:18882.
23. Pilgrim RLC. The aquatic larva and the pupa of *Choristella Philpotti* Tillyard,1917 (Mecoptera: Nannochoristidae). Pacific Insects. 1972;14:151–68.
24. Oertel E. Metamorphosis in the honeybee. J Morphol. 1930;50:295–339.
25. Lowe T, Garwood RJ, Simonsen TJ, Bradley RS, Withers PJ. Metamorphosis revealed: time-lapse three-dimensional imaging inside a living chrysalis. J R Soc Interface. 2013;10:20130304.
26. Wipfler B, Schneeberg K, Löffler A, Hünefeld F, Meier R, Beutel RG. The skeletomuscular system of the larva of *Drosophila melanogaster* (Drosophilidae, Diptera) – a contribution to the morphology of a model organism. Arthropod Struct Dev. 2013;42:47–68.

27. Ge, S.-Q. Hua Y, Ren J, Ślipiński A, Heming B, Beutel RG, et al. Transformation of head structures during the metamorphosis of *Chrysomela populi* (Coleoptera: Chrysomelidae). Arthropod Syst Phylo. 2015;73:129–52.
28. Saltin BD, Haug C, Haug JT. How metamorphic is holometabolous development? Using microscopical methods to look inside the scorpionfly (*Panorpa*) pupa. Spixiana. 2016;39:105–18.
29. Zhao C, Wang M, Gao C, Li M, Zhang K, Yang D, et al. Evolution of holometaboly revealed by developmental transformation of internal thoracic structures in a green lacewing *Chrysopa pallens* (Neuroptera: Chrysopidae). Insect Sci. 2022;29:767–82.
30. Raś M, Wipfler B, Dannenfeld T, Iwan D. Postembryonic development of the tracheal system of beetles in the context of aptery and adaptations towards an arid environment. PeerJ. 2022;10:e13378.
31. Liu S-P, Yin H-D, Li W-J, Qin Z-H, Yang Y, Huang Z-Z, et al. The morphological transformation of the thorax during the eclosion of *Drosophila melanogaster* (Diptera: Drosophilidae). Insects. 2023;14:893.
32. Wipfler B, Machida R, Müller B, Beutel RG. On the head morphology of Grylloblattodea (Insecta) and the systematic position of the order, with a new nomenclature for the head muscles of Dicondylia. Syst Entomol. 2011;36:241–66.
33. Kinnamon SC, Kammer AE, Kiorpes AL. Control of ventilatory movements in the aquatic insect *Corydalus cornutus*: central effect of hypoxia. Physiol Entomol. 1984;9:19–28.

34. Barclay A, Portman RW, Hill PSM. Tracheal gills of the dobsonfly larvae, or hellgrammite *Corydalus cornutus* L. (Megaloptera: Corydalidae). J Kansas Entomol Soc. 2005;78:181–85.
35. Kinnamon SC, Kammer AE. Neural control of ventilatory movements in the aquatic insect *Corydalus cornutus*: the motor pattern. J Comp Physiol A. 1983;153:543–55.
36. Álvarez HA, Tierno de Figueroa JM, Cebada-Ruiz JA. Do Neotropical adult dobsonflies (Megaloptera: Corydalidae) feed on solid material in nature? information from a gut content study. Aquat Insect. 2023;44:205–12.
37. Elgar M, Zhang D, Wang Q, Wittwer B, Pham HT, Johnson TL, et al. Insect antennal morphology: the evolution of diverse solutions to odorant perception. Yale J Biol Med. 2018;91:457–69.
38. Beutel RG, Friedrich F. Comparative study of larval head structures of Megaloptera (Hexapoda). Eur J of Entomol. 2008;105:917–38.
39. Friedrich F, Beutel RG. The thorax of Zorotypus (Hexapoda, Zoraptera) and a new nomenclature for the musculature of Neoptera. Arthropod Struct Dev. 2008;37:29–54.

Supplementary Files

This is a list of supplementary files associated with this preprint. Click to download.

- SupplementaryInformation.docx
- videoS1RhythmicmovementsofgilltuftsduringstationaryrespirationinthefinalinstarlarvaeofProtohermesxanthodes.mp4
- videoS2TheswimmingvideooffinalinstarlarvaeofProtohermesxanthodes.mp4
- videoS3ThefeedingandlocomotionvideooffinalinstarlarvaeofProtohermesxanthodes.mp4